Field dependence of the E1′ and M3′ electron traps in inductively coupled Ar plasma treated *n*-Gallium Arsenide

A. Venter,[1,a)] C. Nyamhere,[1] J. R. Botha,[1] F. D. Auret,[2] S. M. M. Coelho,[2] and W. E. Meyer[2]
[1]*Department of Physics, Nelson Mandela Metropolitan University, P.O. Box 77000, Port Elizabeth 6031, South Africa*
[2]*Department of Physics, University of Pretoria, Lynnwood Road, Pretoria 0002, South Africa*

(Received 23 January 2012; accepted 29 March 2012; published online 1 May 2012)

Inductively coupled Ar plasma etching of n-type (Si doped) Gallium Arsenide (GaAs) introduces several electron traps, $E_c - 0.04$ eV (labelled E1′), $E_c - 0.19$ eV, $E_c - 0.31$ eV, $E_c - 0.53$ eV, and $E_c - 0.61$ eV (behaving like the well documented M3 and labelled M3′ in this study), of which the metastable defects $E_c - 0.04$ eV (E1′), and $E_c - 0.07$ eV are novel. Furthermore, E1′ and M3′ exhibit strong field enhanced carrier emission. Double-correlation deep level transient spectroscopy was used to investigate the field dependent emission behaviour of these two defects. It is shown that for both traps, the observed enhanced emission is due to phonon assisted tunnelling. The latter observation is contrary to the literature reports suggesting that enhanced carrier emission for M3 occurs via the Poole-Frenkel mechanism. *© 2012 American Institute of Physics*.
[http://dx.doi.org/10.1063/1.4709390]

I. INTRODUCTION

Gallium Arsenide (GaAs) remains an important semiconductor material for a wide range of modern electronic applications including high frequency transistors, x-ray and gamma-ray detectors, and photovoltaics.[1,2] Recently, a GaAs triple-junction solar cell with an efficiency of 42.3% at 406 suns has been reported, endorsing the technological importance of GaAs.[3] Although comprehensively studied, new defects are occasionally added to the existing "carrier trap database," while some identified defects and defect complexes are still not well understood. A case in point is the M3/M4 metastable defect complex, initially detected by Buchwald and co-workers[4,5] in GaAs grown by metal-organic vapor phase epitaxy (MOVPE), which may be more thought-provoking than initially anticipated. This defect complex was subsequently also detected by Tabata *et al.*[6] in similar material grown under high V/III ratios. These authors assigned this defect to a complex involving As interstitials, expected to form when an As overpressure is employed during growth. Leitch *et al.*[7] instead reported the M3/M4 defect complex to involve hydrogen and showed that the metastable transformation between the two stable states obeyed first order kinetics.

Irradiation and plasma induced defects in GaAs have been studied extensively[8–13] but to our knowledge no report on the formation of the M3/M4 defect complex by particle irradiation, other than hydrogen plasma treatment, has been reported. Following etching of MOVPE grown *n*-GaAs surfaces with low energy (~60 eV) inductively coupled (Ar) plasmas (ICP), it was recently shown that, apart from two defects not previously observed in GaAs, a defect complex similar to M3/M4 is also introduced.[14,15]

For many defects, the ionization probability and consequently the emission rate are strongly field dependent and will be determined by the perturbation of the potential well by the applied electric field.[16] This field dependent emission rate has become a useful tool for probing the physical properties of the potential well to which a carrier is confined (i.e., the structure of the defect). Three mechanisms describing this observed enhancement have been proposed: (i) the Poole-Frenkel (PF) effect, which occurs for charged defect states only, (ii) phonon-assisted tunnelling (PAT), and (iii) direct tunnelling (DT), both occurring for defects in all charged states. Direct tunnelling is predominant when electric fields exceeding 8×10^7 V/m are present in the space charge region of a Schottky barrier diode (SBD) or *pn*-junction, usually only relevant in highly doped semiconductors.[17]

This paper reports on the field dependent emission behaviour of two defects $E_c - 0.04$ eV and $E_c - 0.61$ eV (M3′) recently detected in ICP (Ar) etched *n*-GaAs. The Poole-Frenkel and Karpus-Perel phonon assisted tunnelling model, tailored, and employed by Ganichev *et al.*,[18] are used in this study to establish the mechanisms responsible for the observed emission enhancement pertaining to these defects. It is shown that for both defects, emission is enhanced through coupling of the defect with lattice vibrations of energy lower than the binding energy of the electron to the defect, i.e., phonon assisted tunnelling. (Note: The primed labelling scheme (M3′ and M4′) refers to defects observed following Ar ICP etching, while un-primed labels (M3 and M4) refer to similar (and possibly the same) defects reported in the literature).

II. EXPERIMENTAL

Si doped (100) *n*-type epitaxial GaAs layers (5 μm) grown by metal organic vapour deposition (MOVPE) on n^+ GaAs substrates were used in this study. The average free carrier density (N_d) of the material, specified by the supplier (SPIRE Semiconductor) and confirmed by standard

a)Authors to whom correspondence should be addressed. Electronic mail: andre.venter@nmmu.ac.za. Tel.: +27(0)415042579. Fax: +27(0)415041989.

capacitance-voltage (C-V) measurements at 1 MHz, was $1.0 \times 10^{15}\,\text{cm}^{-3}$. The samples were diced into approximately 2.5 mm × 5 mm rectangles. Following this, organic contaminants were removed by standard cleaning procedures described in detail elsewhere.[14,15] Immediately after cleaning, ohmic contacts were formed by depositing Ni-AuGe-Ni (50 Å:1500 Å:450 Å) on the backside of the n^+ substrate, followed by annealing at 450 °C for 2 min in a 99.999% pure Ar atmosphere in order to minimize the contact resistance. Prior to SBDs fabrication, 10 min Ar plasma etches were performed using a Copra DN200 inductively coupled plasma beam source. The energy and fluence rate of the plasma ions were 60 eV and $10^{15}\,\text{cm}^{-2}\,\text{s}^{-1}$, respectively. The samples were again briefly etched and deoxidized before circular Pd SBDs, 0.6 mm in diameter and 100 nm thick, were evaporated onto the front surface of the samples. For assessment purposes, a reference sample, not exposed to the plasma, was also prepared.

Laplace deep level transient spectroscopy (LDLTS) (Ref. 19) was used to study the electric field dependent emission behaviour of the defects. For this purpose two transients, related to filling pulses V_p and $V_p + \delta V$, respectively, were independently obtained and subtracted from one another to yield a difference DLTS (DDLTS) spectrum. This ensured that emission was obtained from approximately the same defect population located in a "narrow slice" between x_p and $x_p + \delta x_p$ (corresponding to V_p and $V_p + \delta V$) of the depletion region throughout the field dependent measurement. The field was adjusted by maintaining a constant pulse difference, δV (0.25 V in this study), while varying the reverse bias between 1 V and 4 V. The temperature dependent defect emission rate was obtained from the difference spectra by LDLTS, while the defect signatures were extracted from Arrhenius plots in the conventional manner using,[20]

$$e_n = \sigma_{na}\gamma_n T^2 e^{-(E_c - E_T/kT)}. \quad (1)$$

Here, e_n is the electron emission rate at a given temperature T, σ_{na} is the apparent capture cross section of the defect, k is the Boltzmann constant and γ_n equal to $(N_c\langle v_n\rangle^2)g_0/g_1$ has the value $2.21 \times 10^{20}\,\text{cm}^{-2}\,\text{s}^{-2}\,\text{K}^{-2}$ for an electron trap in GaAs.[21] N_c is the density of states in the conduction band, $\langle v_n\rangle$ is the average thermal velocity of the electrons, and g_0 and g_1 are degeneracy terms related to the defect state before and after electron emission.

Ganichev *et al.*[18] suggested a simple criterion to distinguish between the one-dimensional (1-D) Poole-Frenkel effect and phonon-assisted tunnelling. Regarding the former mechanism (PF), a linear dependence between $\ln(e)$ and $\sqrt{E}$ should exist, whereas for phonon assisted tunneling, the relationship between $\ln(e)$ and E^2 should be linear. These criteria were employed in this study to establish the mechanism/s involved in the observed field enhanced emission for the defects E_c – 0.04 eV and E_c – 0.61 eV, respectively.

III. RESULTS AND DISCUSSION

Prior to the presentation and subsequent interpretation of results, it is instructive to discuss some theoretical aspects regarding field emission in advance. The Poole-Frenkel effect is expected to dominate field enhanced carrier emission from a trap in the depletion region of a reverse biased SBD or *pn*-junction under low field conditions ($<10^5$ V/m).[18] Emission occurring via this effect from a 1-D columbic well is quantified by the following equation:[22,23]

$$e(E) = e(0)\exp^{\beta\sqrt{E}/kT}, \quad (2)$$

where e(0) is the charge emission rate in the absence of an electric field, $\beta = (q^3/\pi\varepsilon)^{1/2}$ and q, ε, k, and T have their usual meaning.

According to Ganichev *et al.*[18,24,25] phonon assisted tunnelling, possible for defects in all charge states, will dominate for moderate electric fields (10^7 – 10^8 V/m) and the logarithm of the emission rate should depend linearly on the square of the applied electric field. The model put forward by Karpus and Perel for phonon assisted tunnelling yielded the following analytical expression for the field dependent emission rate:[18]

$$e(E) = e(0)\exp^{E^2/E_c^{*2}}, \quad (3)$$

where E_c, the characteristic field strength, is given by

$$E_c = \sqrt{\frac{3m^*\hbar}{q^2\tau_2^{*3}}}, \quad (4)$$

m* is the effective mass, q is the elementary charge, and τ_2 is the tunnelling time

$$\tau_2 = \frac{\hbar}{2k_B T} \mp \tau_1. \quad (5)$$

According to the Huang-Rhys model,

$$\tau_1 = \frac{1}{2\omega_{vib}}\left|\ln\left(\frac{\varepsilon_T}{\varepsilon_{opt} - \varepsilon_T}\right)\right|. \quad (6)$$

τ_1 is a time constant related to the inverse localized impurity vibrational frequency. ε_T and ε_{opt} are the thermal and optical ionization energies of the defect, respectively. The ∓ sign corresponds to the adiabatic potential structures of substitutional impurities and auto localized centers, respectively. (It is instructive to note that gradually changing external conditions, the applied electric field in this case permits a defect to alter its configuration causing the emission rate to change. If the system starts in a particular initial eigenstate of Hamiltonian H_i, it will evolve to a corresponding final eigenstate of Hamiltonian H_f, adapting its form to the changing conditions, $|\langle x|\psi(t_f)\rangle|^2 \neq |\langle x|\psi(t_i)\rangle|^2$. The time associated with this evolution is related to the characteristic tunnelling time, $\tau_1 = t_f - t_i$).

Fig. 1(a) depicts a DLTS spectrum of the defects detected following Ar ICP etching. Several electron traps, E_c – 0.04 eV (labelled E1′), E_c – 0.19 eV, E_c – 0.31 eV (M4), E_c – 0.53 eV, and E_c – 0.61 eV (possibly the well documented M3), were introduced. The reference did not contain any defects within the detection limit of the system between 20 K

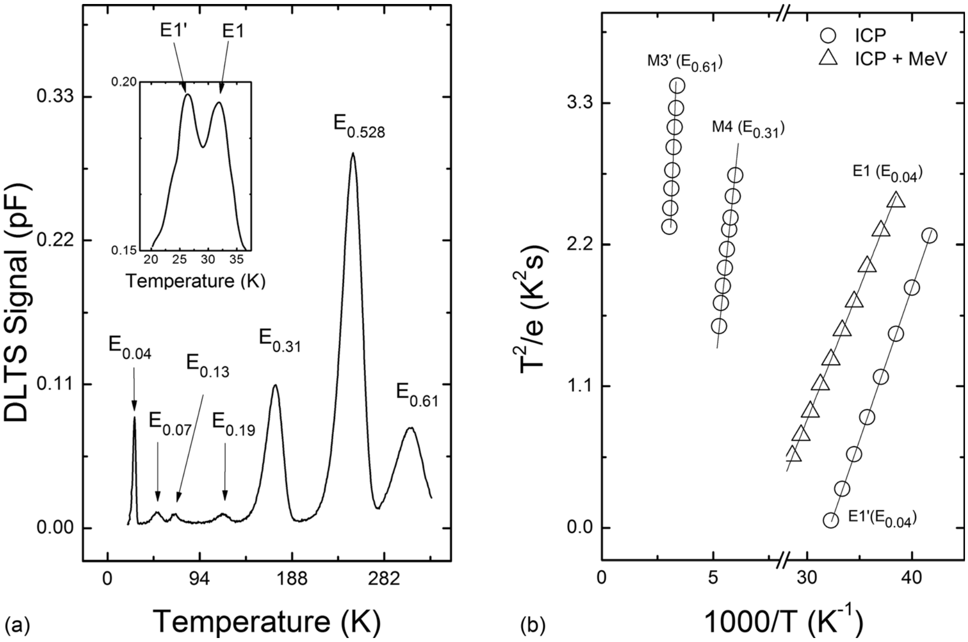

FIG. 1. (a) DLTS spectrum of the defects detected in ICP Ar etched *n*-GaAs. The inset shows the same sample (from 20 K to 35 K) following MeV electron irradiation using a Sr^{90} source. Evidently Ar ICP etching introduced a defect unrelated to the well documented E1. (b) DLTS Arrhenius plots of the defects pertinent to this study.

and 320 K. The inserted figure shows a spectrum acquired between 20 K and 35 K for a sample exposed to Ar ICP etching followed by MeV electron irradiation using a Sr^{90} source. The defect labelled E1′, similar in temperature position to E1 (related to β-irradiation), is detected around 25 K. Evidently, two distinct defects are detected following MeV electron irradiation confirming that Ar plasma etching introduces a defect not previously identified and generally mistaken for E1. A detailed report on this topic has recently been published.[14,15] Fig. 1(b) shows the DLTS Arrhenius plots from which the trap signatures of the defects relevant to this study, viz., E1′, E1, M3, and M4 were extracted. Of these, only E1′ and $E_c - 0.61$ eV (M3′) exhibited field enhanced emission. It is instructive to note that both these defects exhibit metastability with M3′ being one stable state of the M3′/M4′ complex detected following ICP etching. The metastable counterpart for E1′ has not yet been detected.

In a previous study, it has been shown that E1′ can be introduced by applying a reverse bias of –2 V (RBA) at 400 °C for 10 min and removed under zero bias annealing (ZBA) at 390 °C for 60 min.[14,15] It is also interesting to note that E1′ is introduced when M3 is removed. The transformation kinetics for E1′ is currently being investigated.

Fig. 2 shows the emission rate of electrons from traps (a) E1′ and (b) M3′ as a function of the applied electric field present in the depletion region of the reverse biased SBD for temperatures ranging between 29 K and 33 K in the case of E1′ and 310 K and 320 K for M3′. The latter defect is well studied and believed to be one component (M3) of the M3/M4 metastable defect complex frequently observed in hydrogen containing/exposed GaAs.[5,7,26,27] The applied reverse bias ranged from 1 V to 4 V, translating to maximum space charge electric fields of between 1×10^4 V/m and 3×10^4 V/m. Evidently, electron emission is enhanced

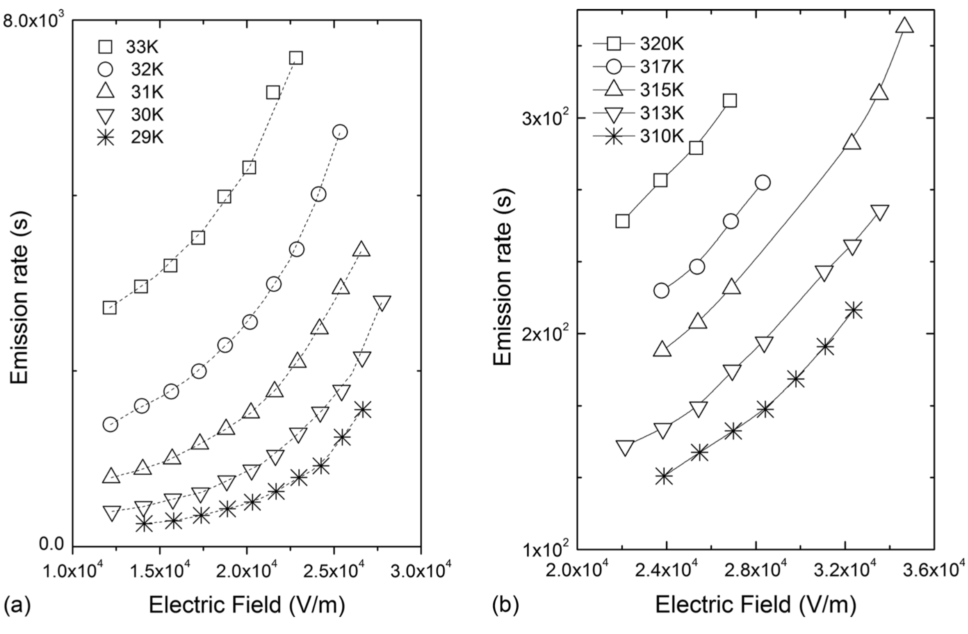

FIG. 2. Emission rate dependence on the applied electric field for the electron trap (a) E1′ and (b) M3′, respectively, as determined from LDLTS measurements using the double pulse technique (difference DLTS). The applied reverse bias ranged between 1 V and 4 V.

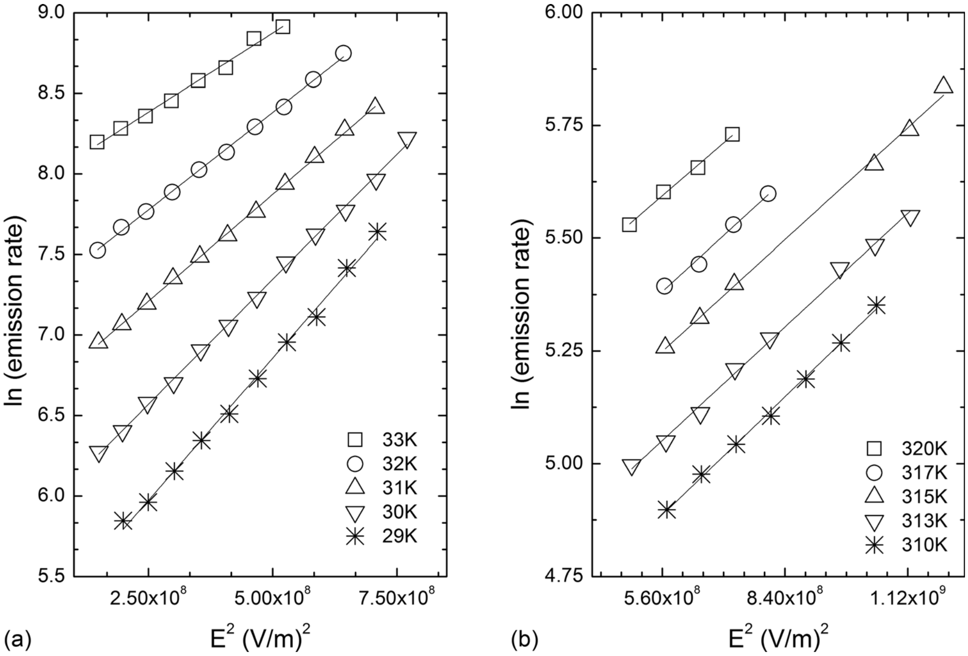

FIG. 3. The linear dependence of the logarithm of the emission rate for (a) trap E1′ and (b) trap M3′ on the square of the electric field for five different temperatures. The solid lines correspond to a fit of $e(E) = e(0)\exp^{E^2/E_c^2}$ from which the characteristic field and consequently the tunnelling time, τ_2 were determined.

non-linearly by the application of increasing electric fields for both these defects and since a plot of ln*(e)* is not proportional to $E^{0.5}$, enhanced emission is not due to the Poole-Frenkel mechanism (not shown).

Fig. 3 shows the linear dependence of ln*(e)*, obtained at different temperatures, on the square of the electric field E^2 for defects E1′ and M3′, respectively. It is consequently concluded that phonon assisted tunnelling is the mechanism responsible for the observed field enhanced emission. Phonon assisted tunnelling as quantified by Eq. (3) permits the calculation of a characteristic field E_c (such that $\ln[e(E)/e(0)] = E^2/E_c^2$ equals unity) and the tunnelling time (τ_2) for this process. This is done by linearizing equation (3) and extracting the slope $(1/E_c^2)$, which in turn is related to τ_2 via Eq. (4). Equation (5) was subsequently used to determine τ_1, the time constant (described earlier) associated with the enhanced field emission observed for each of the two traps.

Fig. 4 shows the temperature dependence of the characteristic tunnelling time (τ_2) for (a) E1′ and (b) M3′, respectively. Values for τ_1 of -5.83×10^{-13} s^{-1} for E1′ and -1.15×10^{-13} s^{-1} for M3′ were obtained. Both E1′ and M3′ are consequently identified as a negatively charged auto localized or a neutral defect center. Various authors reported emission enhancement for M3, but in all reports, the Poole-Frenkel mechanism is believed to be predominant for this defect.[5,28] Manifestation of the Poole-Frenkel effect generally suggests a donor-like trap, whereas the absence thereof is interpreted as the trap being acceptor-like. Importantly, the situation may be slightly more complex. Field enhancement may be impeded if a trap has a high barrier for capture, i.e., if capture is slow, enhanced

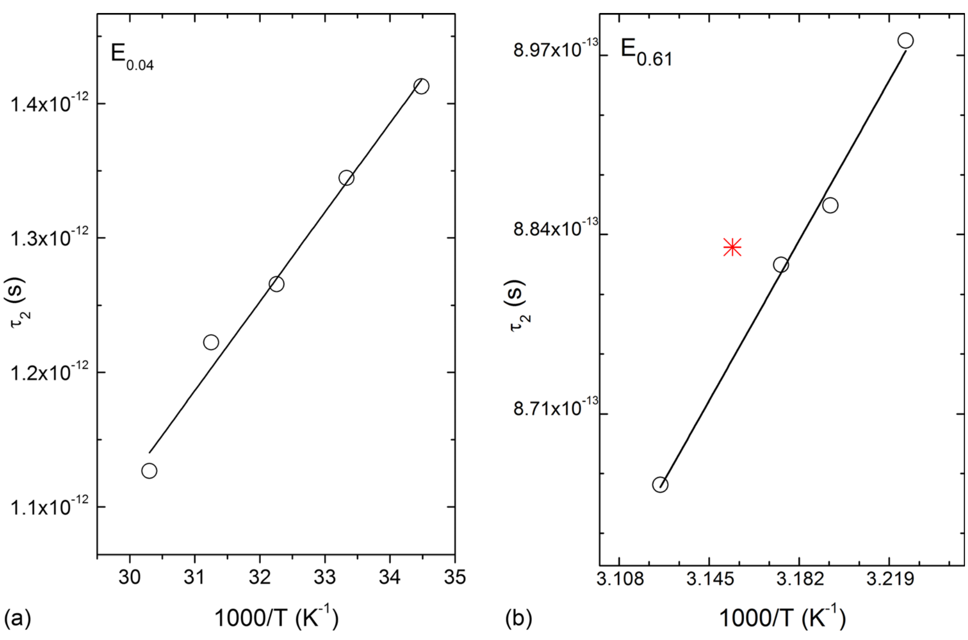

FIG. 4. Temperature dependence of the characteristic tunnelling time (τ_2) for (a) E1′ and (b) M3′. The symbols represent the experimentally obtained values and the solid lines a fit to these for the purpose of extracting τ_1. The star represents a data point, omitted in the fit (solid line).

emission may not be detectable. The absence of the Poole-Frenkel effect should therefore be interpreted carefully. Notably, field enhanced emission was not observed for the M4′ defect in this study. This result correlates with observation made for this defect in similar studies and supports the view that it probably is acceptor-like.

IV. CONCLUSIONS

The field dependence of defects detected in epitaxial *n*-GaAs following ICP (Ar) etching has been investigated. Two electron traps, E1′ (E_c – 0.04 eV) and M3′ (E_c – 0.61 eV), exhibited field dependent carrier emission. In both cases, the logarithm of the emission rate was found to dependent linearly on the square of the electric field for the range of the electric field and temperature investigated, suggesting that the observed enhancement is well described by the models proposed for phonon assisted tunnelling. According to the literature, the enhanced carrier emission observed for the M3 trap occurs via the Poole-Frenkel mechanism which is in contrast with results obtained in this study for M3′. The time constant for E1′ and M3′ was found to be -5.83×10^{-13} s^{-1} and -1.15×10^{-13} s^{-1}, respectively. Both E1′ and M3′ are consequently identified as a negatively charged (or neutral) auto localized defect center.

ACKNOWLEDGMENTS

This work is based upon research supported by the SA Research Chairs Initiative of the Department of Science and Technology and the National Research Foundation, the Nelson Mandela Metropolitan University and the University of Pretoria.

[1]"Semiconductor for room temperature nuclear detectors applications," in *Semiconductor and Semimetal Series*, edited by T. E. Schlesinger and R. B. James (Academic, San Diego, CA, 1995), Vol. 43, chap. 10.
[2]M. Cuzin, R. B. James, P. F. Manfredi, and P. Siffert, Nucl. Instrum. Methods **A380**, 255–262 (1996).
[3]See www.pvtech.org/news/gaas_solar_cell_from_spire_sets_42.3_conversion_efficiency_record.
[4]W. R. Buchwald, N. M. Johnson, and L. P. Trombetta, Appl. Phys. Lett. **50**, 1007 (1987).
[5]W. R. Buchwald, G. J. Gerardi, E. H. Poindexter, N. M. Johnson, H. G. Grimmeiss, and D. J. Keeble, Phys. Rev. B **40**, 2940 (1989).
[6]A. S. Tabata, M. A. A. Pudensi, and A. M. Machado, J. Appl. Phys. **65**, 4076 (1989).
[7]A. W. R. Leitch, Th. Prescha, and J. Weber, Phys. Rev. B **45**, 14401 (1992).
[8]D. Pons and J. C. Bourgoin, J. Phys. C **18**, 3839 (1985).
[9]F. D. Auret, L. J. Bredell, G. Myburg, and W. O. Barnard, Jpn. J. Appl. Phys. Part 1 **30**, 80 (1991).
[10]S. A. Goodman, F. D. Auret, and W. E. Meyer, Nucl. Instrum. Methods Phys. Res. B **90**, 349 (1994).
[11]F. Zhan, J. Hu, Y. Zhang, and F. Lu, Appl. Surf. Sci. **255**, 8257 (2009).
[12]J. M. Borrego, R. J. Gutmann, and S. Ashok, IEEE Trans. Nucl. Sci. NS23, 1671 (1976).
[13]C. Nyamhere, J. R. Botha, and A. Venter, Physica B **406**, 2273 (2011).
[14]F. D. Auret, P. J. Janse van Rensburg, W. E. Meyer, S. M. M. Coelho, Vl. Kolkovsky, J. R. Botha, C. Nyamhere, and A. Venter, Physica B **407**, 1497 (2012).
[15]A. Venter, F. D. Auret, C. Nyamhere, J. R.Botha, P. J. Janse van Rensburg, W. E. Meyer, S. M. M. Coelho, and Vl. Kolkovsky, J. Appl. Phys. **111**, 13703 (2012).
[16]T. Tsarova, T. Wosinski, A. Makosa, and Z. Tkaczyk, Semicond. Sci. Technol. **24**, 105021 (2009).
[17]G. Vincent, A. Chantre, and D. Bois, J. Appl. Phys. **50**, 5484 (1979).
[18]S. D. Ganichev, E. Ziemann, W. Prettl, I. N. Yassievich, A. A. Istratov, and E. R. Weber, Phys. Rev. B **61**, 10361 (2000).
[19]L. Dobaczewski, P. Kaczor, I. D. Hawkins, and A. R. Peaker, J. Appl. Phys. **76**, 194 (1994).
[20]P. J. Wang, T. F. Kuech, M. A. Tishler, P. M.Mooney, G. Scilla, and F. Cardone, J. Appl. Phys. **64**, 4975 (1988).
[21]D. K.Schroder, *Semiconductor Material and Device Characterization* (John Wiley & Sons, New York, 1990), chap. 7.
[22]J. Frenkel, Phys. Rev. **54**, 647 (1938).
[23]J. Bourgoin and M. Lannoo, *Point Defects in Semiconductors. II: Experimental Aspects*, edited by J. Bourgoin and M. Lannoo (Springer-Verlag, Berlin and Heidelberg, 1983).
[24]S. D. Ganichev, W. Prettl, and P. G. Huggard, Phys. Rev. Lett. **71**, 3882 (1993).
[25]S. D. Ganichev, W. Prettl, and I. N. Yassievich, Phys. Solid State **39**, 1703 (1997).
[26]A. B. Conibear, A. W. R. Leitch, and C. A. B. Ball, Phys. Rev. B **47**, 1846 (1993).
[27]G. Pfeiffer and J. Weber, Mater. Sci. Forum **143**, 873 (1994).
[28]Y. Tokuda, K. Kamiya, and T. Okumura, J. Cryst. Growth **210**, 260 (2000).